TITLE: The Molecular and Structural Asymmetry of the Plasma Membrane

AUTHORS: Lorent JH[1], Ganesan L[1], Rivera-Longsworth G[2], Sezgin E[3], Levental KR[1], Lyman E[4], Levental I[1,*]

AFFILIATIONS: [1]McGovern Medical School, Department of Integrative Biology and Pharmacology, University of Texas Health Science Center at Houston

[2]Biological Sciences Department, Columbia University

[3]John Radcliffe Hospital, Weatherall Institute of Molecular Medicine, University of Oxford

[4]Department of Physics and Astronomy; Department of Chemistry and Biochemistry, University of Delaware

*Corresponding author / lead contact: ilya.levental@uth.tmc.edu ; orcid: 0000-0002-1206-9545

ABSTRACT: A fundamental feature of cellular plasma membranes (PM) is the asymmetric distribution of lipids between the bilayer leaflets. This asymmetry is central to cellular physiology, regulating signaling, apoptosis, coagulation, and cell-cell fusion. While the broad transbilayer distributions of some lipid types are well established, the detailed lipidomic asymmetry of the PM has not been characterized and thus the compositions of the individual leaflets remain poorly understood. Further, how these compositional differences contribute to structural asymmetries between PM leaflets in living cells is not defined. Here, we report the distinct lipidomes and biophysical properties of both monolayers in living mammalian PMs. Using mass spectrometry coupled to enzymatic digestion, we report the detailed compositions of PM leaflets of human erythrocytes. We find a dramatic asymmetry in phospholipid unsaturation, with the cytoplasmic leaflet being ~2-fold more unsaturated than the exoplasmic. Atomistic simulations of lipid mixtures compiled from the lipidomic observations suggested significant asymmetries in lipid order, packing, and dynamics between the two PM leaflets. These were probed directly in the PM of living cells by Fluorescence Lifetime Imaging Microscopy (FLIM) of leaflet-selective, environment-sensitive probes. The outer PM leaflet is highly packed and ordered, resembling a liquid ordered phase, whereas the inner leaflet is significantly more disordered. This biophysical asymmetry is maintained in the endocytic system. These observations reveal the detailed compositional and biophysical asymmetry of mammalian plasma membranes, elucidating fundamental design principles of living membranes.

SIGNIFICANCE STATEMENT: The asymmetric distribution of lipids between the two bilayer leaflets is a fundamental feature of mammalian plasma membranes. Here, we quantify the comprehensive lipidomes of the two PM leaflets in living mammalian cells and examine their consequences on leaflet physical properties. Using computer simulations, we predict distinct biophysical features for the two leaflets and confirm these with a variety of spectroscopic and microscopic techniques. We find that the outer leaflet of the membrane contains many more fully saturated lipids, which endows it with higher lipid packing and lower diffusivity.

INTRODUCTION

The asymmetric distribution of lipids between the two leaflets of the plasma membrane (PM) bilayer is a prevalent and fundamental feature of cells across the tree of life (1-3). In mammals, compositional asymmetry is most widely

studied for phosphatidylserine (PS), a negatively charged lipid found almost exclusively on the cytoplasmic (inner) leaflet of the PM. Other phospholipid headgroups are also asymmetrically distributed, with sphingolipids enriched in the exoplasmic leaflet, while charged and amino-phospholipids are more abundant on the cytoplasmic side (2, 4, 5). These distributions were originally established in red blood cells (RBCs) (4, 5) and platelets (6), later confirmed in PMs of various nucleated cell types (1, 7), and also proposed in organellar membranes (8). Direct measurements of lipid asymmetries in biomembranes have been limited to the few major lipid types defined by their polar headgroups. However, advances in lipidomics reveal a vast diversity of lipid species in mammalian membranes, which are comprised of hundreds of lipid species with distinct headgroups, acyl chains, and backbone linkages (9). It is unknown how these species are distributed across the PM, and thus the compositions of the individual leaflets remain poorly understood. Similarly, the asymmetries of intracellular organellar membranes are not known.

Functional membrane phenotypes are strictly dependent on the emergent physical properties of lipid collectives, including membrane fluidity, permeability, lipid packing, intrinsic curvature, bending stiffness, surface charge, transbilayer stress profiles, and lateral domain formation(10). Thus, one of the most important and challenging questions in membrane biology concerns the biophysical consequences of membrane asymmetry. While the connections between membrane composition and physical properties have been addressed extensively in studies of symmetric bilayers, little is known about how these insights translate to compositionally asymmetric membranes. Recently, robust protocols for producing asymmetric synthetic membranes (11, 12) have been developed and used to characterize coupling (or lack thereof) across the bilayer (13-15), the effects of lipid asymmetry on protein conformation (11, 12), and the influence of proteins on lipid distribution between leaflets (16). The extent to which membrane properties are coupled across the bilayer in living cells remains one of the foremost open questions in cell biology.

Disparities in biophysical properties between the two leaflets of the PM in living cells have long been proposed (17), but remain ambiguous due to experimental limitations and inconsistencies. Studies have often relied on RBCs, since they lack internal membranes, and exoplasmic quenchers or headgroup-specific chemistries to probe individual leaflets. However, even these seemingly simple methods yielded contradictory conclusions, with some studies inferring a more fluid inner PM leaflet[18,19](18, 19) and others a more fluid outer leaflet (20-25). Ultimately, the presence and nature of biophysical asymmetry in mammalian membranes remains unresolved because of several limitations inherent to methodologies that rely on lipid-based probes and fluorescence quenchers (see Supplementary Text). Finally, previous studies have focused almost exclusively on the PM, which is amenable to analysis by virtue of being the most accessible membrane in the cell, and the only one in erythrocytes and platelets. Whether biophysical asymmetries are present in intracellular organelles has been rarely studied and remains unknown.

Here, classical approaches are combined with modern analytical tools to investigate the lipidomes and biophysical properties of both leaflets in intact mammalian PMs. Using enzymatic digestion, the asymmetric distribution of ~400 lipid species is defined for human RBC PMs and compiled into a detailed, comprehensive model for the compositions of PM leaflets. While the observed headgroup distributions are largely in line with previous reports, a striking asymmetry is observed for phospholipid acyl chains, with the cytoplasmic leaflet composed largely of highly unsaturated lipids. These observations suggested asymmetric properties in the two leaflets of the PM, an inference that was confirmed by atomistic simulations of complex lipid bilayers. These predictions were then directly examined using a novel approach that relies on selective staining of PM leaflets by a leaflet-selective, environment-sensitive

fluorescent reporter. A clear difference in lipid packing is observed between the exo- and cytoplasmic leaflets of a living cell PM, wherein a tightly packed outer leaflet apposes a more loosely packed inner leaflet, with these biophysical asymmetries persisting in intracellular endosomes.

RESULTS

Detailed lipidomic asymmetry of a mammalian plasma membrane

The asymmetric distribution of phospholipid headgroups in eukaryote PMs was described by classical studies on mammalian red blood cells and platelets (4-6), and then confirmed in various mammalian cell types (1, 7), as well as yeast (26) and nematodes (27). However, the differences in phospholipid backbones and acyl chains between exo- and cytoplasmic leaflets of the PM have not been investigated. Combining phospholipase digestion with modern lipidomics, we report the detailed, comprehensive lipidomic asymmetry of the human red blood cell (RBC) plasma membrane. To this end, RBCs were treated with either phospholipases or sphingomyelinase to specifically digest only the lipid species present on the exoplasmic leaflet of the PM. Detailed, comprehensive lipidomics of ~400 unique phospholipid species remaining after enzymatic digestion reveals the composition of the inner leaflet, while the digested lipids were inferred to comprise the outer leaflet (Fig 1A and Supp Data). Independent enzyme treatments and extensive controls (see Supplementary Figs 1-2 and Supp Methods) allowed us to quantify the comprehensive lipidomes of both leaflets. The measured asymmetric lipid headgroup distributions (Fig 1A) were consistent with classical estimates (4, 5). PLA2 treatment of intact cells minimally affected PE or PS, consistent with the near-absolute inner leaflet confinement of these aminophospholipids reported previously (4-6). PI, PA, and PE-O were similarly unaffected, suggesting their near-complete inner leaflet residence. All of these classes were completely degraded by treatment of sonicated RBCs (Fig S1). SM was largely degraded (~90%) by treatment of intact cells with SMase, confirming its concentration in the outer leaflet, while ~60% of the PC was on the outer leaflet.

Analysis of lipid hydrophobic chains revealed a striking difference in acyl chain unsaturation between leaflets, with almost 40% of exoplasmic leaflet phospholipids being saturated (not including the sphingoid backbone double bond) and the majority having less than 2 unsaturations per lipid (Fig 1B). In contrast, the cytoplasmic leaflet was highly enriched in lipids with polyunsaturated acyl chains, with the majority of lipids containing 4 or more unsaturations. Overall, the average outer leaflet lipid bears 1.6 unsaturations in comparison to 3.4 on the inner leaflet (Fig 1B, inset). Most of the lipid headgroup classes were confined to one of the PM leaflets, precluding any within-class asymmetry. The only exception present at high content in both leaflets was PC, which showed a surprisingly asymmetric distribution: fully saturated PC species (e.g. dipalmitoyl PC) were almost exclusively present on the *cytosolic* leaflet, whereas exoplasmic PC showed a preference for polyunsaturated species (Fig 1C). More generally, there was a clear correlation between the unsaturation of PC species and their relative enrichment in the outer leaflet (Fig 1D).

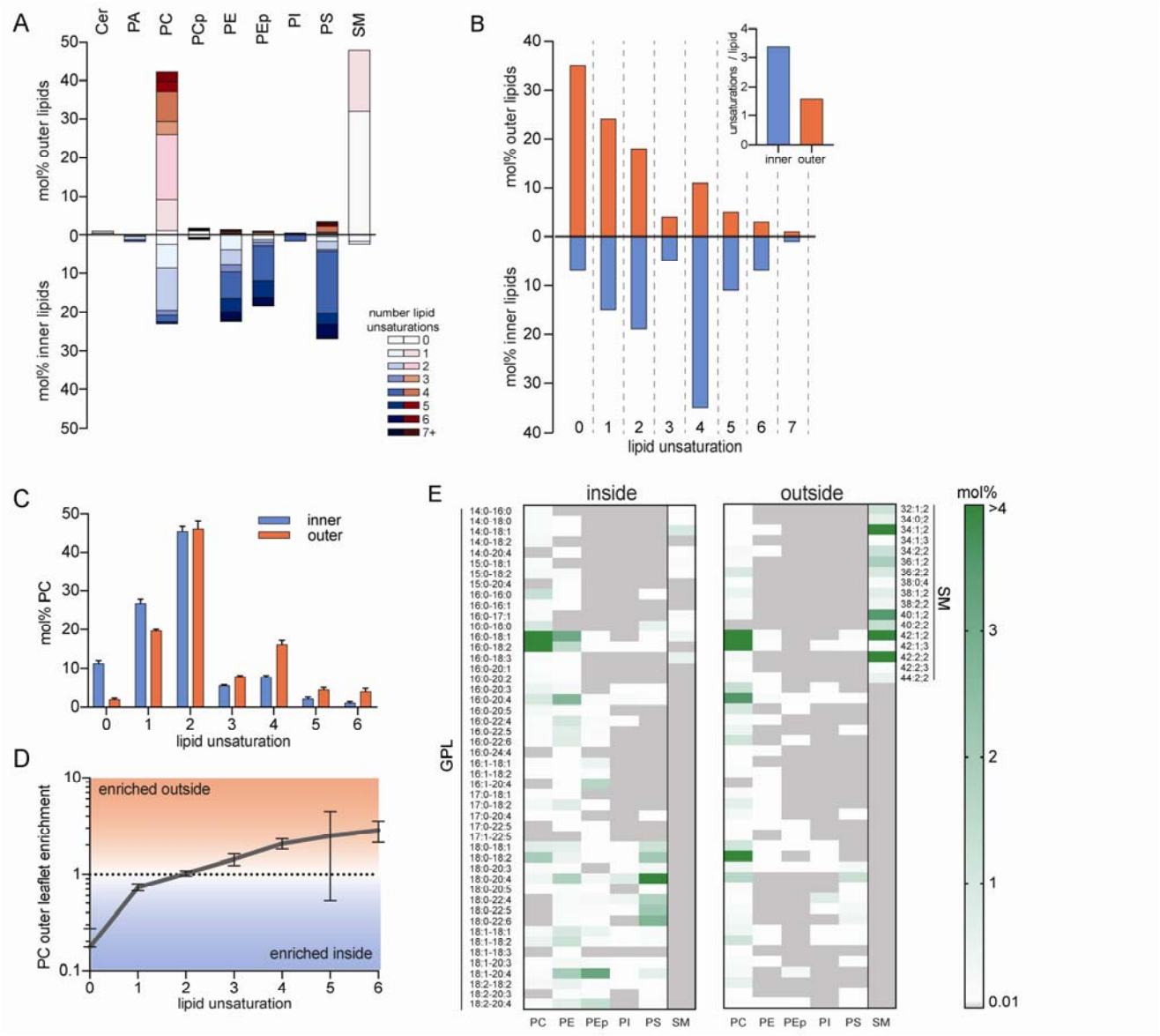

Fig 1 - Lipidomic asymmetry of erythrocyte PMs. (A) Phospholipid compositions of exo- (red) and cytoplasmic (blue) PM leaflets as defined by enzymatic digestion and mass spectrometry. The exoplasmic leaflet is almost exclusively composed of PC and SM; the inner leaflet is approximately equimolar between PC, PE, PS, and PEp. (B) Leaflet asymmetry of acyl chain unsaturation. The plurality of phospholipids in the outer leaflet are fully saturated, whereas the majority of the cytoplasmic leaflet is polyunsaturated. (inset) Abundance-weighted average unsaturation is ~2-fold greater for inner leaflet phospholipids. (C) Asymmetry of acyl chain saturation in PM PC. Fully saturated acyl chains are highly enriched in the inner leaflet PC and there is a (D) general correlation between outer leaflet enrichment of PC species and the extent of unsaturation. (E) Lipidomic bar codes of the inner and outer PM leaflets. Mol% of lipid species are encoded in the intensity of color (darkest = most abundant).

The comprehensive phospholipid compositions ('lipidomic barcode') of the two leaflets are shown in Fig 1E (Supp Data) and summarized in Fig 2A&C. These data unequivocally establish several previously overlooked or under-emphasized features: (1) the lipidome is dominated by 'hybrid' lipids (i.e. one saturated and one unsaturated acyl chain), with the notable exception of highly saturated SM comprising ~35% of outer leaflet PLs; (2) polyunsaturated

lipids comprise two-thirds of inner leaflet PLs; (3) ~33% of outer leaflet PLs are SMs bearing very-long chain (24:0 and 24:1) fatty acids. (4) lipids containing two unsaturated acyl chains are rare, comprising ~10% of the inner leaflet and essentially not present on the outer leaflet; (5) ether linked lipids (i.e. plasmalogens) comprise a sizeable fraction (~20%) of the inner leaflet; (6) there is clear headgroup selectivity for lipid acyl chains, with polyunsaturated fatty acids concentrated in PE and PS and wholly excluded from SM; (7) the major PC species on the outer leaflet bear di-unsaturated acyl chains.

Table I – Distilled inner and outer leaflet lipidomes of the RBC PM.

(A) Outer leaflet

representative	mol% of
PC 16:0-18:2	22.2
SM 34:1;2	22.4
SM 42:2;2	18.5
SM 42:1;2	14.4
PC 16:0-20:4	9.7
PC 18:0-18:1	8.4
PC 18:1-18:2	2.0
PS 18:0-20:4	1.5
PI 18:0-22:4	0.9

(B) Inner leaflet

representative	mol% of
PS 16:0-20:4	33.1
PE O- 18:1-22:4	13.7
PC 16:0-18:2	13.0
PE 16:0-22:6	11.9
PE 18:1-20:4	6.9
PC 16:0-18:1	7.0
PE 16:0-18:1	4.8
PE O- 18:2-20:4	3.7
PC 16:0-16:0	2.9
SM 34:1;2	2.0
PI 18:0-20:4	1.0

Atomistic simulations demonstrate differences in leaflet physical properties

The striking differences in phospholipid composition between PM leaflets suggested the possibility of biophysical asymmetries across the PM. Differences in membrane properties associated with lipid headgroups (e.g. charge and size) have been extensively documented (28-33), but lipid acyl chains are also major determinants of membrane structure and organization (10). Namely, membranes rich in saturated lipids are more tightly packed, rigid, and ordered, whereas high unsaturation levels yield more fluid, loosely packed membranes, suggesting that the outer leaflet of mammalian PMs may be more tightly packed and ordered than the inner leaflet. This possibility was evaluated by atomistic molecular dynamics simulations (34). To specifically isolate the biophysical effects of distinct leaflet compositions from transbilayer asymmetry *per se*, we compared symmetric bilayers composed of inner- or outer-mimetic lipid complements (Table I). The full lipidomic complexity described in Fig 1 was distilled to a set of representative lipids for each leaflet that recapitulates the headgroup and acyl chain profiles of the compete leaflet lipidomes (Fig 2A&B; Table I; for details, see Supp Table II). Cholesterol was included in both systems at 40 mol%, since this was the abundance observed in RBCs overall, and cholesterol was found to distribute approximately equally between leaflets in previous PM-mimetic simulations (35) (cholesterol asymmetry is addressed in Discussion).

To quantitatively compare the two systems, we measured bulk parameters that reflect experimental measurements of membrane order, diffusivity, and headgroup packing. Overall lipid order was assessed by calculating the

concentration-weighted average acyl chain order parameters (($\bar{S}_{CD}$) along both hydrophobic chains for all lipids in the systems (e.g. Fig S3). The outer leaflet-mimetic was roughly twice as ordered as the inner leaflet (Fig 2D), consistent with the inner leaflet being rich in relatively disordered unsaturated acyl chains. These differences were also reflected in the order parameters of identical lipids in the two mixtures, with 1-palmitoyl-2-linoleoyl PC (16:0/18:2 PC) and palmitoyl-SM being more ordered in the outer leaflet mixture (Fig S3). This order disparity corresponded to different molecular areas for various lipids comprising the inner versus outer leaflet simulations. The overall area per phospholipid (APL) was greater in the inner leaflet versus outer leaflet (59 versus 55 $Å^2$), as also reflected in the APL for individual lipid species common to both simulations (Fig 2G). Finally, we observed striking differences in membrane fluidity, as the diffusion coefficient ($D_{leaflet}$) (calculated from concentration-weighted mean square displacements (MSDs) of all lipids in the simulation) was ~2-fold greater in the inner compared to the outer leaflet (Fig 2E). Finally, to explore differences in lipid packing at the headgroup level, hydrophobic packing defects were measured in the two systems. Such defects are regions of the membrane where hydrophobic acyl chains are transiently exposed to water(36). The defect distribution is clearly shifted in the inner leaflet, indicating more abundant and larger packing defects, reflective of reduced headgroup packing (Fig 2F).

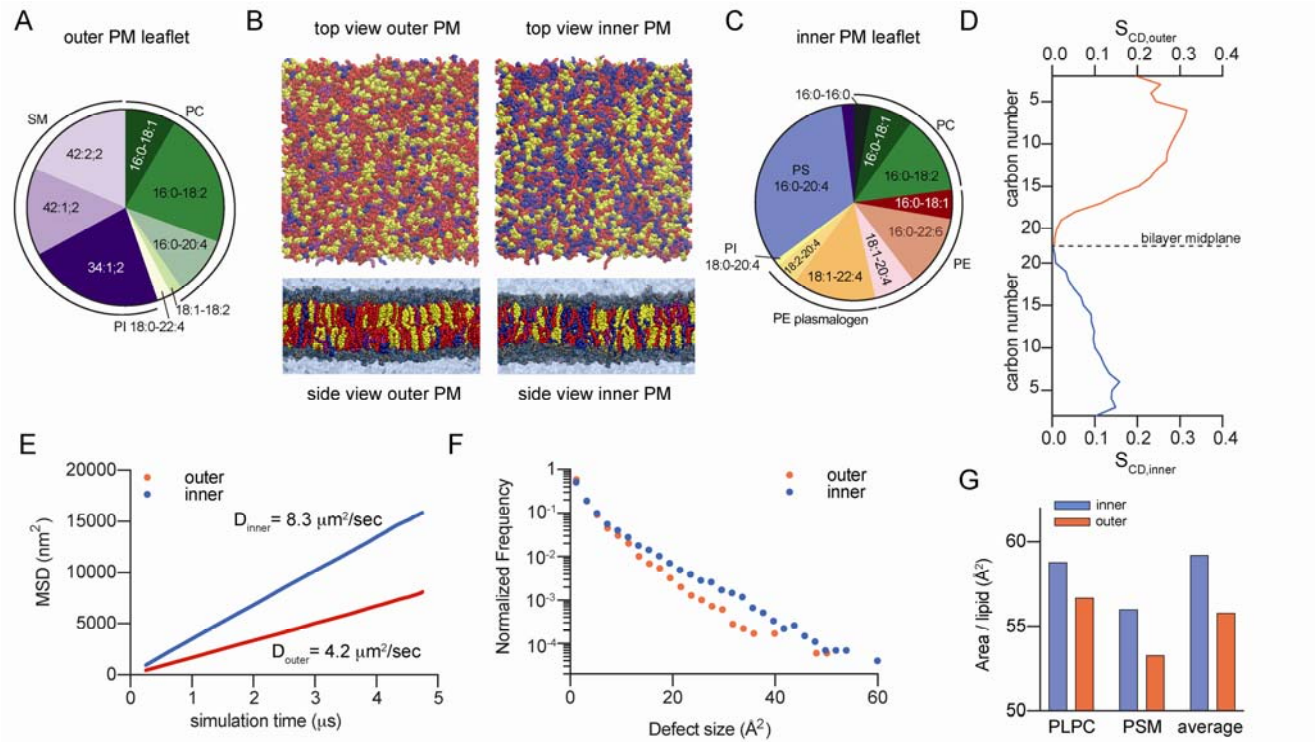

Fig 2 – Atomistic simulation of biophysical asymmetry of erythrocytes PM. (A) Compiled compositions of inner and outer PM leaflets from lipidomics. (B) Final snapshots of outer- and inner-PM leaflet mimetic simulations (yellow = cholesterol, red = saturated acyl chains, purple = mono- and di-unsaturated, blue = polyunsaturated; headgroups not shown in top views). (C) Concentration-weighted average order parameters for lipids in the outer versus inner leaflet simulation suggest a more ordered outer leaflet. (D) Slope of average MSD over time reveals ~2-fold slower diffusivity of the simulated outer leaflet. (E) Histogram of hydrophobic defects reveals more abundant large defects in the simulated inner leaflet. (F) Area/phospholipid for PLPC and PSM (the two lipids shared between both simulations) and the abundance-weighted average phospholipid.

PM leaflets have distinct biophysical properties

The atomistic simulations predict that membranes composed of inner leaflet lipids would have different physical properties from outer leaflet, as suggested by various experimental observations of broadly similar membranes. However, such insights have largely been based on investigations of symmetric membranes, as methodologies for robustly constructing asymmetric model membranes have only recently become widely accessible (11, 15, 37, 38). Thus, the biophysical consequences of acyl chain asymmetry in either model or biological membranes remain poorly explored. The biophysical asymmetry of live cell PMs was probed using a fluorescent reporter of membrane packing (Di-4-ANEPPDHQ, Di4) (Fig. S5A). The photophysical characteristics (e.g. fluorescence lifetime and emission spectra) of this dye are dependent on lipid packing (39-44), making it a robust reporter of membrane properties. The key feature making it suitable for leaflet-selective measurements is the presence of two charged moieties (Fig S5A) that prevent passive flip-flop across the bilayer (40). Thus, the exoplasmic leaflet of living cells can be selectively stained by adding the dye directly to the extracellular solution, whereas the inner leaflet is selectively stained by microinjecting the dye into the cytoplasm (schematized in Fig 3A). These features were confirmed in extensive control experiments described in the Supplement.

Having definitively confirmed Di4 as a leaflet-selective indicator of membrane physical properties, we probed their asymmetry in the PMs in two cultured mammalian cell types (RBLs and 3T3 fibroblasts). In both, microinjecting Di4 broadly stained intracellular membranes, with the PM easily identifiable both by the general morphology of the cell and the higher Di4 lifetime in the PM compared to internal membranes (left column of Fig 3B-C), revealing that the cytoplasmic leaflet of the PM is more tightly packed than those of intracellular membranes. An intensity-weighted histogram (right column) of a PM mask (middle column) revealed an average lifetime (τ_{Di4}) of ~2.5 ns in microinjected cells (Fig 3A-C, top row). When the same cells were then stained externally with Di4, the lifetime of the internal membranes was unaffected (Fig S6), whereas the Di4 lifetime in the PM increased significantly (Fig 3A-C, middle row), suggesting that the exoplasmic PM leaflet is more tightly packed than the cytoplasmic leaflet. This inference was confirmed by comparison to cells stained only from the outside, where Di4 signal was confined to the PM (absence of flipping prevents translocation to the cytosol, while short incubations prevent significant endocytosis). In outside-only stained cells (Fig 3A-C, bottom row), Di4 lifetime in the PM was ~3.2 ns, significantly greater than the PM in microinjected cells, revealing a striking asymmetry in membrane packing between the inner and outer leaflet. Similar values and trends were observed for both cell types (Fig 3D). To relate τ_{Di4} values to membrane properties, the cellular measurements were compared with those of L_o and L_d phases of synthetic phase-separated GUVs (Fig S4). The outer leaflets of cellular PMs were slightly less packed than the synthetic L_o phase, whereas the inner leaflets were approximately intermediate between the L_o and L_d phases. To test the computational prediction that inner leaflet components diffuse faster than outer (Fig 2E), Fluorescence Correlation Spectroscopy (FCS) was used to evaluate the diffusion of fluorescent proteins anchored either to the outer leaflet (GPI-GFP) or inner leaflet (SH4 domain fused to mNeonGreen; SH4-mNG) by saturated fatty acids. Outer leaflet-anchored GPI-GFP diffused ~2-fold slower than inner leaflet SH4-mNG, in quantitative consistency with the computational result.

These measurements strongly suggest a biophysical asymmetry in mammalian PMs, with the outer leaflet being less fluid and more tightly packed. To rule out any artifacts associated with microinjection or the presence of internal

membranes in nucleated cells, we investigated biophysical asymmetry in human erythrocyte PMs. These cells are too small for efficient microinjection, thus only the outer leaflet was probed by external staining. To assess biophysical asymmetry, asymmetric PMs in untreated RBCs were compared with those where asymmetry was pharmacologically abrogated. Specifically, treatment with phorbol myristate acetate (PMA) induces efficient PM scrambling, which is detected by the exposure of PS on the exoplasmic leaflet via the PS-binding probe Annexin V (AnxV) (45). This effect was confirmed, as untreated RBCs were almost exclusively AnxV-negative, whereas PMA-treated RBCs were uniformly AnxV-positive (Fig 3F, left column). Outer leaflet packing was significantly reduced by lipid scrambling, suggesting that the inner leaflet of the RBC PM is more loosely packed than the outer (Fig 3F-G). NR12S, a complementary leaflet-selective order-sensitive probe, showed similar trends, ruling out probe-specific effects (Fig S9).

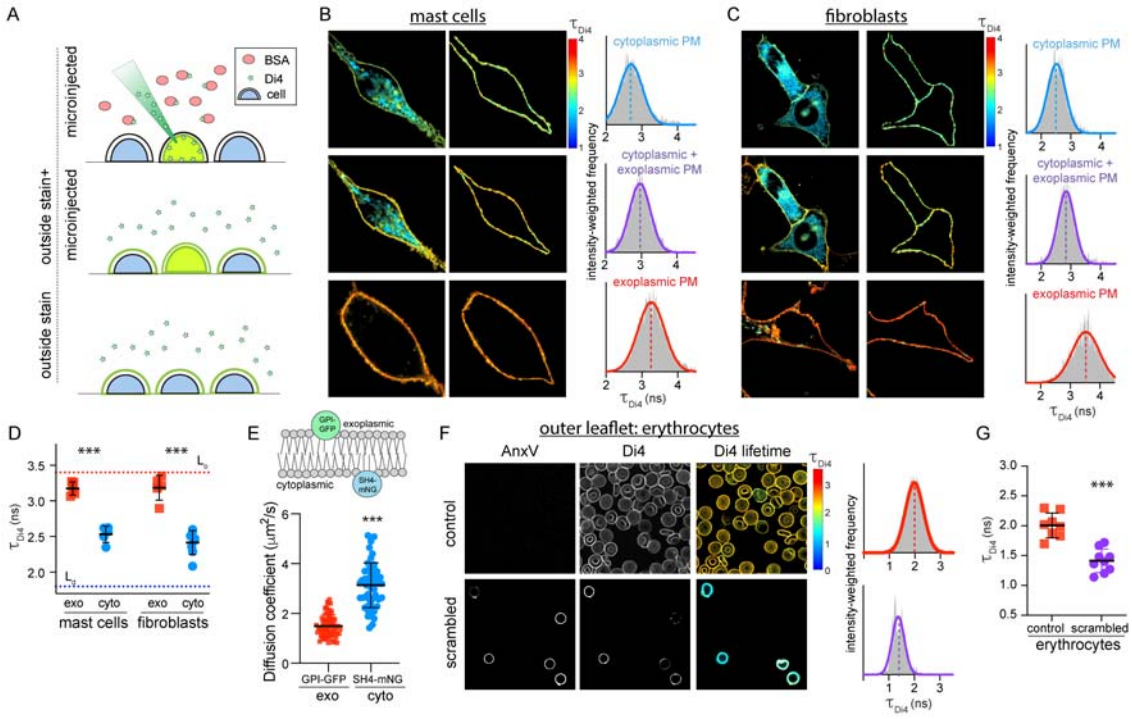

Figure 3 – Biophysical asymmetry of the PM. (A) Microinjection of Di4 in presence of BSA stains only the cytoplasmic PM leaflet (microinjected). Subsequent addition of Di4 to the outside stains both membrane leaflets (outside stain + microinjected). Staining from the outside labels only the outer PM monolayer (outside stain). Exemplary FLIM images of (B) RBL mast cells and (C) 3T3 fibroblasts showing (left) whole cells, (middle) PM masks, and (right) intensity-weighted histograms of the PM mask. (D) Average Di4 lifetime in exoplasmic (red) versus cytoplasmic (blue) PM leaflets. Dotted lines represent Di4 lifetime in L_o and L_d phases in GUVs. (E) Diffusion coefficients measured by FCS of exoplasmically anchored GPI-GFP (red) versus cytoplasmically anchored SH4-mNG (blue) (F) AnxV staining for exoplasmic PS (left), Di4 intensity and lifetime (middle), and lifetime histogram (right), in control versus PMA-scrambled erythrocytes stained from the outside with Di4. PMA-induced scrambling induces PS exposure (AnxV binding) and reduces the packing of the outer leaflet. (G) Average Di4 lifetime in untreated (red)

versus scrambled (purple) PM outer leaflets in erythrocytes. ***p<0.001 one-way ANOVA between groups; representative of at least 3 independent experiments.

Lipid packing asymmetry is preserved upon endocytosis

Having observed differential packing between the two PM leaflets, we next investigated whether biophysical asymmetries persist in endocytic membranes, which are composed in part of material arriving from the PM, but are also remodeled to comprise compartments for sorting, processing, and degradation (46). To probe the biophysical asymmetry in the endocytic system, these compartments were marked by pulse-chase with fluorescent dextran. Cells were incubated with fluorescent dextran for 2 h, during which the dextran is taken up by passive pinocytosis and accumulates in endocytic compartments, which were expanded by the increased load of non-degradable material (Fig 4A). The outer leaflets of cell PMs were then labelled by external Di4 (as in Fig 3), and the cells were incubated for up to 1 h (without Di4 or dextran) to allow dye endocytosis and staining of endolysosome membrane lumenal leaflets (Fig 4A). The contours of the dextran staining were then used as an endolysosomal membrane mask, which was overlaid onto the Di4 FLIM image (Fig 4A, mask). Strikingly, the Di4 lifetime in endocytic organelles was only slightly reduced compared to the outer PM leaflet (Fig 4). In contrast, the cytoplasmic leaflets of the same dextran-positive endosomes probed by Di4 microinjection had a much lower membrane packing (i.e. τ_{Di4}) than any of the lumenally stained endosomes. With longer incubation times, there was a slight reduction of τ_{Di4} in the lumenally labelled endosomes, likely due to membrane remodeling during endocytic maturation (Fig 4B). These observations were completely consistent between cell types (RBLs in Fig 4; fibroblasts in Fig S10), and imply that biophysical membrane asymmetry is maintained in the endosomal system.

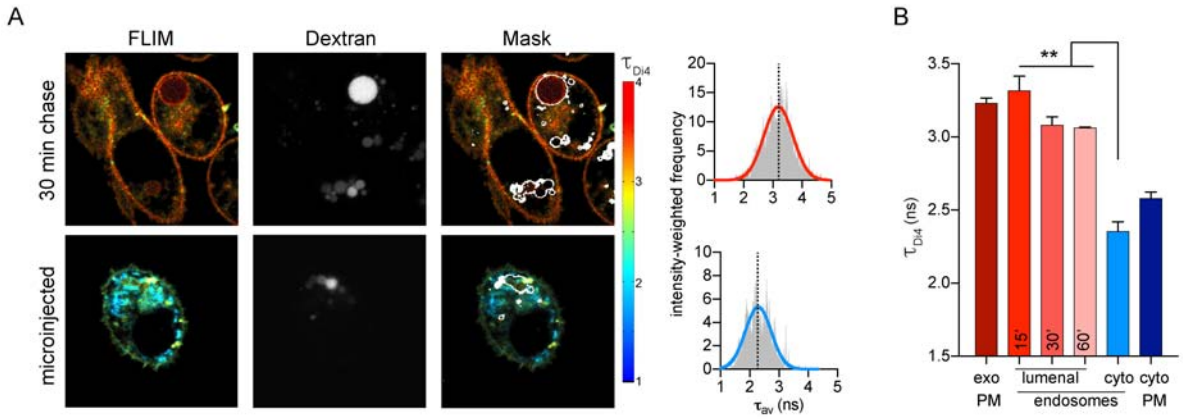

Figure 4 – Asymmetry of membrane packing through the endocytic pathway. (A) Exemplary FLIM images of Di4 lifetime and dextran fluorescence following 30 min incubation to "chase" stains into endosomes. The accumulation of dextran (middle) is used to create an endosomal membrane mask (right images) to derive intensity-weighted histograms of τ_{Di4} (right). (B) The high lifetime (i.e. lipid packing) of the exoplasmic PM leaflet is maintained in the luminal leaflets of endosomes, even up to 60 min after endocytosis.

DISCUSSION

Combining enzymatic digestion with quantitative mass spectrometry revealed the detailed lipidomes of the inner and outer leaflets of RBC PMs. Consistent with expectations (2, 4, 5), SMs were highly enriched on the outer leaflet, whereas most glycerophospholipids were exclusive to the cytoplasmic leaflet, excepting PCs, which were distributed approximately equally between the two leaflets. The quantitative accuracy of these measurements is supported by several key controls: (1) complete digestion of target lipids in lysed cells (Fig S1); (2) lack of hemoglobin leakage in enzyme-treated cells (Fig S2); and (3) decrease in target lipids (e.g. SM) that quantitatively matches stoichiometric appearance of reaction products (e.g. Cer; Fig S1). The third point is crucial, as the target and product lipids use different standards and often different detection modes (e.g. positive versus negative ion) for quantification. The excellent correspondence between the amount of target eliminated and product formed supports the quantitative accuracy of our assay. Although this enzymatic approach cannot evaluate the lipid asymmetry of cells which contain internal membranes, isolated PM lipidomes from such cells (47, 48) could be used to predict leaflet lipidomes, relying on the well supported assumption (49, 50) that headgroup classes would have similar asymmetries as measured here in RBCs.

It is important to point out that the reported compositions are not fully comprehensive. Complex glycolipids are not detected in the shotgun platform, nor are phosphorylated inositols. The most abundant glycolipid in human RBCs is globoside (Gb4), estimated to be <5% of all lipids(51); PIP_2 is the most abundant phosphoinositide, estimated at <1%(52). Similarly, while the total concentration of cholesterol is quantified (~40 mol%), its distribution between leaflets is not accessible by our methodology and remains controversial (53). Classical measurements found conflicting results (23, 54), and these contradictions are mirrored in more recent work, with some groups reporting inner leaflet enrichment of cholesterol (55, 56) and others the opposite (57). Our measurements do not directly inform on this debate, though the higher packing of the outer leaflet may argue for higher cholesterol content therein. However, the packing of the inner leaflet is such that extremely low cholesterol concentrations are also unlikely. In the absence of consensus, and because cholesterol can rapidly flip between leaflets (58-60), the molecular dynamics simulations (Fig 2) assumed no *a priori* cholesterol preference for either leaflet.

The most notable disparity found between the acyl chains in the two RBC PM leaflets is ~2-fold more double bonds per lipid in the inner versus outer leaflet (Fig 1B). This difference is likely responsible for the robust biophysical PM asymmetry we observe in RBCs and several nucleated mammalian cell types (Fig 3, Fig S8-9). The biophysical asymmetry appears to persist after internalization of the PM into the early endosomal pathway, suggesting that lipid asymmetry persists in some intracellular compartments, consistent with other reports (61). These live cell results are consistent with model membrane observations suggesting that lipid order can be decoupled between the two leaflets of asymmetric membranes (14, 62).

Comparing the lifetime of Di4 in the PM leaflets of live cells to synthetic model membranes suggests that the outer PM leaflet has biophysical properties similar to a L_o phase, whereas the inner PM leaflet is intermediate between the ordered and disordered phases (Fig 3 & S4). This comparison prompts examination of long-standing questions about the physical organization of the mammalian PM and its partitioning into ordered domains termed lipid rafts (63). Recent model membranes experiments revealed that ordered domains in phase-separating leaflets can induce domains in apposed leaflets which otherwise would not form L_o phases (37, 64, 65). Long-chain SM species are implicated as central mediators of such transbilayer domain coupling (37). The asymmetric RBC lipidome reveals an outer leaflet rich in high-melting lipids (i.e. saturated SM) and cholesterol, with a non-trivial abundance of low melting lipids (i.e.

unsaturated glycerophospholipids). Such a membrane monolayer is poised to form coexisting ordered and disordered domains (66-68), with an area fraction dominated by the ordered phase. The inner leaflet contains largely low-melting unsaturated lipids that are not amenable to ordered domain formation, though the high abundance of long-chain SM species in the outer leaflet may promote domain coupling between leaflets. The ultimate organization of the membrane is then a combination of these membrane-intrinsic effects and extrinsic inputs like protein scaffolds (69) and cytoskeletal dynamics (70, 71).

The ubiquitous asymmetry of PMs in eukaryotic organisms prompts a key question: what adaptive advantage is gained from PM asymmetry? The generation and maintenance of lipid disparities in the two leaflets is likely energetically costly, suggesting a significant benefit to maintaining their highly asymmetric distribution. Several hypothetical explanations are possible: from the material properties standpoint, coupling distinct leaflets may combine desirable features into a single bilayer. For example, a tightly packed outer leaflet may serve as an effective permeability barrier, while the more fluid inner leaflet allows for rapid signal transmission. A non-exclusive alternative is that PM asymmetry is used for energy storage, in analogy with energy storage by pumped-storage hydroelectricity. Cells may store the potential energy generated by pumping lipids against their concentration gradients, to be released later upon regulated scrambling of the bilayer. Finally, membrane asymmetries could be used as organellar identifiers for selective sorting of lipids and proteins. Deciphering the ultimate purpose of membrane asymmetry is central to understanding the functions of cell membranes.

List of Supplementary Materials
Materials and Methods
Figure S1-S11
Supplementary Discussion
Tables S1 and S2
Supplementary References
Supplementary Data – Asymmetric lipidomes

Acknowledgements: All fluorescence microscopy was performed at the Center for Advanced Microscopy, Department of Integrative Biology & Pharmacology at McGovern Medical School, UTHealth. We gratefully acknowledge Milka Doktorova, Kai Simons, Theodore Steck, Yvonne Lange, and Gerald Feigenson for their critical feedback on this manuscript. Funding for this work was provided by the NIH/National Institute of General Medical Sciences (GM114282, GM124072, GM120351), the Volkswagen Foundation (grant 93091), and the Human Frontiers Science Program (RGP0059/2019). ES is funded by Newton-Katip □elebi Institutional Links grant (352333122). Anton2 computer time was provided by the National Resource for Biomedical Supercomputing (NRBSC), the Pittsburgh Supercomputing Center (PSC), and the Biomedical Technology Research Center for Multiscale Modeling of Biological Systems through grant P41GM103712-S1 from the National Institutes of Health. All authors have no competing interests.

Author contributions: JHL, IL, EL, and KRL designed the study. JHL, KRL, LG, GR, and ES performed experiments. EL performed and analyzed the molecular dynamics simulations. JHL, KRL, and IL analyzed the experimental results and wrote the paper. None of the authors have any competing interests.

References

1. Devaux PF (1991) Static and dynamic lipid asymmetry in cell membranes. *Biochemistry* 30(5):1163-1173.
2. Op den Kamp JA (1979) Lipid asymmetry in membranes. *Annu Rev Biochem* 48:47-71.
3. Barsukov LI, Kulikov VI, Bergelson LD (1976) Lipid transfer proteins as a tool in the study of membrane structure. Inside-outside distribution of the phospholipids in the protoplasmic membrane of Micrococcus lysodeikticus. *Biochem Biophys Res Commun* 71(3):704-711.
4. Bretscher MS (1972) Asymmetrical lipid bilayer structure for biological membranes. *Nature: New biology* 236(61):11-12.
5. Verkleij AJ, *et al.* (1973) The asymmetric distribution of phospholipids in the human red cell membrane. A combined study using phospholipases and freeze-etch electron microscopy. *Biochim Biophys Acta* 323(2):178-193.
6. Schick PK, Kurica KB, Chacko GK (1976) Location of phosphatidylethanolamine and phosphatidylserine in the human platelet plasma membrane. *The Journal of clinical investigation* 57(5):1221-1226.
7. Sandra A, Pagano RE (1978) Phospholipid asymmetry in LM cell plasma membrane derivatives: polar head group and acyl chain distributions. *Biochemistry* 17(2):332-338.
8. Bollen IC, Higgins JA (1980) Phospholipid asymmetry in rough- and smooth-endoplasmic-reticulum membranes of untreated and phenobarbital-treated rat liver. *Biochem J* 189(3):475-480.
9. Klose C, Surma MA, Simons K (2013) Organellar lipidomics--background and perspectives. *Curr Opin Cell Biol* 25(4):406-413.
10. Janmey PA, Kinnunen PK (2006) Biophysical properties of lipids and dynamic membranes. *Trends in cell biology* 16(10):538-546.
11. Lin Q, London E (2014) The influence of natural lipid asymmetry upon the conformation of a membrane-inserted protein (perfringolysin O). *J Biol Chem* 289(9):5467-5478.
12. Cheng HT, Megha, London E (2009) Preparation and properties of asymmetric vesicles that mimic cell membranes: effect upon lipid raft formation and transmembrane helix orientation. *J Biol Chem* 284(10):6079-6092.
13. Chiantia S, Schwille P, Klymchenko AS, London E (2011) Asymmetric GUVs prepared by MbetaCD-mediated lipid exchange: an FCS study. *Biophys J* 100(1):L1-3.
14. Chiantia S, London E (2012) Acyl chain length and saturation modulate interleaflet coupling in asymmetric bilayers: effects on dynamics and structural order. *Biophys J* 103(11):2311-2319.
15. Heberle FA, *et al.* (2016) Subnanometer Structure of an Asymmetric Model Membrane: Interleaflet Coupling Influences Domain Properties. *Langmuir* 32(20):5195-5200.
16. Doktorova M, *et al.* (2019) Gramicidin Increases Lipid Flip-Flop in Symmetric and Asymmetric Lipid Vesicles. *Biophys J*.
17. Sharpe HJ, Stevens TJ, Munro S (2010) A comprehensive comparison of transmembrane domains reveals organelle-specific properties. *Cell* 142(1):158-169.
18. Morrot G, *et al.* (1986) Asymmetric lateral mobility of phospholipids in the human erythrocyte membrane. *Proc Natl Acad Sci U S A* 83(18):6863-6867.
19. el Hage Chahine JM, Cribier S, Devaux PF (1993) Phospholipid transmembrane domains and lateral diffusion in fibroblasts. *Proc Natl Acad Sci U S A* 90(2):447-451.
20. Cogan U, Schachter D (1981) Asymmetry of lipid dynamics in human erythrocyte membranes studied with impermeant fluorophores. *Biochemistry* 20(22):6396-6403.
21. Schroeder F (1978) Differences in fluidity between bilayer halves of tumour cell plasma membranes. *Nature* 276(5687):528-530.
22. Igbavboa U, Avdulov NA, Schroeder F, Wood WG (1996) Increasing age alters transbilayer fluidity and cholesterol asymmetry in synaptic plasma membranes of mice. *Journal of neurochemistry* 66(4):1717-1725.
23. Schachter D, Abbott RE, Cogan U, Flamm M (1983) Lipid fluidity of the individual hemileaflets of human erythrocyte membranes. *Annals of the New York Academy of Sciences* 414:19-28.
24. Nikolova-Karakashian MN, Petkova H, Koumanov KS (1992) Influence of cholesterol on sphingomyelin metabolism and hemileaflet fluidity of rat liver plasma membranes. *Biochimie* 74(2):153-159.
25. Rimon G, Meyerstein N, Henis YI (1984) Lateral mobility of phospholipids in the external and internal leaflets of normal and hereditary spherocytic human erythrocytes. *Biochim Biophys Acta* 775(3):283-290.
26. Alder-Baerens N, Lisman Q, Luong L, Pomorski T, Holthuis JC (2006) Loss of P4 ATPases Drs2p and Dnf3p disrupts aminophospholipid transport and asymmetry in yeast post-Golgi secretory vesicles. *Mol Biol Cell* 17(4):1632-1642.
27. Darland-Ransom M, *et al.* (2008) Role of C. elegans TAT-1 protein in maintaining plasma membrane phosphatidylserine asymmetry. *Science* 320(5875):528-531.
28. Yeung T, *et al.* (2008) Membrane phosphatidylserine regulates surface charge and protein localization. *Science* 319(5860):210-213.
29. Zhang W, Crocker E, McLaughlin S, Smith SO (2003) Binding of peptides with basic and aromatic residues to bilayer membranes: phenylalanine in the myristoylated alanine-rich C kinase substrate effector domain penetrates into the hydrophobic core of the bilayer. *J Biol Chem* 278(24):21459-21466.
30. Xu P, Baldridge RD, Chi RJ, Burd CG, Graham TR (2013) Phosphatidylserine flipping enhances membrane curvature and negative charge required for vesicular transport. *J Cell Biol* 202(6):875-886.
31. Wang J, *et al.* (2002) Lateral sequestration of phosphatidylinositol 4,5-bisphosphate by the basic effector domain of myristoylated alanine-rich C kinase substrate is due to nonspecific electrostatic interactions. *J Biol Chem* 277(37):34401-34412.

32. Levental I, Janmey PA, Cebers A (2008) Electrostatic contribution to the surface pressure of charged monolayers containing polyphosphoinositides. *Biophys J* 95(3):1199-1205.
33. Sodt AJ, Venable RM, Lyman E, Pastor RW (2016) Nonadditive Compositional Curvature Energetics of Lipid Bilayers. *Phys Rev Lett* 117(13):138104.
34. Ingolfsson HI, Arnarez C, Periole X, Marrink SJ (2016) Computational 'microscopy' of cellular membranes. *J Cell Sci* 129(2):257-268.
35. Ingolfsson HI, *et al.* (2014) Lipid organization of the plasma membrane. *J Am Chem Soc* 136(41):14554-14559.
36. Cui H, Lyman E, Voth GA (2011) Mechanism of membrane curvature sensing by amphipathic helix containing proteins. *Biophys J* 100(5):1271-1279.
37. Lin Q, London E (2015) Ordered raft domains induced by outer leaflet sphingomyelin in cholesterol-rich asymmetric vesicles. *Biophys J* 108(9):2212-2222.
38. Lin Q, London E (2014) Preparation of artificial plasma membrane mimicking vesicles with lipid asymmetry. *PloS one* 9(1):e87903.
39. Dinic J, Biverstahl H, Maler L, Parmryd I (2011) Laurdan and di-4-ANEPPDHQ do not respond to membrane-inserted peptides and are good probes for lipid packing. *Biochim Biophys Acta* 1808(1):298-306.
40. Jin L, *et al.* (2006) Characterization and application of a new optical probe for membrane lipid domains. *Biophys J* 90(7):2563-2575.
41. Owen DM, Rentero C, Magenau A, Abu-Siniyeh A, Gaus K (2011) Quantitative imaging of membrane lipid order in cells and organisms. *Nat Protoc* 7(1):24-35.
42. Owen DM, *et al.* (2006) Fluorescence lifetime imaging provides enhanced contrast when imaging the phase-sensitive dye di-4-ANEPPDHQ in model membranes and live cells. *Biophys J* 90(11):L80-82.
43. Sezgin E, Sadowski T, Simons K (2014) Measuring lipid packing of model and cellular membranes with environment sensitive probes. *Langmuir* 30(27):8160-8166.
44. Amaro M, Reina F, Hof M, Eggeling C, Sezgin E (2017) Laurdan and Di-4-ANEPPDHQ probe different properties of the membrane. *J Phys D Appl Phys* 50(13):134004.
45. Wesseling MC, *et al.* (2016) Novel Insights in the Regulation of Phosphatidylserine Exposure in Human Red Blood Cells. *Cell Physiol Biochem* 39(5):1941-1954.
46. Diaz-Rohrer BB, Levental KR, Simons K, Levental I (2014) Membrane raft association is a determinant of plasma membrane localization. *Proc Natl Acad Sci U S A* 111(23):8500-8505.
47. Levental KR, *et al.* (2016) Polyunsaturated lipids regulate membrane domain stability by tuning membrane order. *Biophys J* 110(8):1800-1810.
48. Levental KR, *et al.* (2017) omega-3 polyunsaturated fatty acids direct differentiation of the membrane phenotype in mesenchymal stem cells to potentiate osteogenesis. *Science advances* 3(11):eaao1193.
49. Boon JM, Smith BD (2002) Chemical control of phospholipid distribution across bilayer membranes. *Medicinal research reviews* 22(3):251-281.
50. Li G, *et al.* (2016) Efficient replacement of plasma membrane outer leaflet phospholipids and sphingolipids in cells with exogenous lipids. *Proc Natl Acad Sci U S A* 113(49):14025-14030.
51. Yamakawa T, Nagai Y (1978) Glycolipids at the cell surface and their biological functions. *Trends Biochem Sci* 3(2):128-131.
52. Levental I, Cebers A, Janmey PA (2008) Combined electrostatics and hydrogen bonding determine intermolecular interactions between polyphosphoinositides. *J Am Chem Soc* 130(28):9025-9030.
53. Steck TL, Lange Y (2018) Transverse distribution of plasma membrane bilayer cholesterol: Picking sides. *Traffic* 19(10):750-760.
54. Schroeder F, *et al.* (1991) Transmembrane distribution of sterol in the human erythrocyte. *Biochim Biophys Acta* 1066(2):183-192.
55. Courtney KC, *et al.* (2018) C24 Sphingolipids Govern the Transbilayer Asymmetry of Cholesterol and Lateral Organization of Model and Live-Cell Plasma Membranes. *Cell Rep* 24(4):1037-1049.
56. Mondal M, Mesmin B, Mukherjee S, Maxfield FR (2009) Sterols are mainly in the cytoplasmic leaflet of the plasma membrane and the endocytic recycling compartment in CHO cells. *Mol Biol Cell* 20(2):581-588.
57. Liu SL, *et al.* (2017) Orthogonal lipid sensors identify transbilayer asymmetry of plasma membrane cholesterol. *Nat Chem Biol* 13(3):268-274.
58. Lin X, Zhang S, Ding H, Levental I, Gorfe AA (2016) The aliphatic chain of cholesterol modulates bilayer interleaflet coupling and domain registration. *FEBS Lett* 590(19):3368-3374.
59. Bennett WD, MacCallum JL, Hinner MJ, Marrink SJ, Tieleman DP (2009) Molecular view of cholesterol flip-flop and chemical potential in different membrane environments. *J. Am. Chem. Soc.* 131(35):12714-12720.
60. Steck TL, Lange Y (2012) How slow is the transbilayer diffusion (flip-flop) of cholesterol? *Biophys J* 102(4):945-946; author reply 947-949.
61. Iaea DB, Maxfield FR (2017) Membrane order in the plasma membrane and endocytic recycling compartment. *PloS one* 12(11):e0188041.
62. Cheng HT, London E (2011) Preparation and properties of asymmetric large unilamellar vesicles: interleaflet coupling in asymmetric vesicles is dependent on temperature but not curvature. *Biophys J* 100(11):2671-2678.
63. Sezgin E, Levental I, Mayor S, Eggeling C (2017) The mystery of membrane organization: composition, regulation and roles of lipid rafts. *Nat Rev Mol Cell Biol* 18(6):361-374.
64. Collins MD, Keller SL (2008) Tuning lipid mixtures to induce or suppress domain formation across leaflets of unsupported asymmetric bilayers. *Proc Natl Acad Sci U S A* 105(1):124-128.

65. Kiessling V, Crane JM, Tamm LK (2006) Transbilayer effects of raft-like lipid domains in asymmetric planar bilayers measured by single molecule tracking. *Biophys J* 91(9):3313-3326.
66. Veatch SL, Keller SL (2005) Miscibility phase diagrams of giant vesicles containing sphingomyelin. *Phys. Rev. Lett.* 94(14):148101.
67. Veatch SL, Polozov IV, Gawrisch K, Keller SL (2004) Liquid domains in vesicles investigated by NMR and fluorescence microscopy. *Biophys J* 86(5):2910-2922.
68. Heberle FA, Wu J, Goh SL, Petruzielo RS, Feigenson GW (2010) Comparison of three ternary lipid bilayer mixtures: FRET and ESR reveal nanodomains. *Biophys J* 99(10):3309-3318.
69. Kusumi A, *et al*. (2012) Dynamic organizing principles of the plasma membrane that regulate signal transduction: commemorating the fortieth anniversary of Singer and Nicolson's fluid-mosaic model. *Annu. Rev. Cell Dev.Biol*. 28:215-250.
70. Koster DV, Mayor S (2016) Cortical actin and the plasma membrane: inextricably intertwined. *Curr Opin Cell Biol* 38:81-89.
71. Machta BB, Papanikolaou S, Sethna JP, Veatch SL (2011) Minimal model of plasma membrane heterogeneity requires coupling cortical actin to criticality. *Biophys J* 100(7):1668-1677.